# Model-free optical surface reconstruction from deflectometry data

L. R. Graves, H. Choi, W. Zhao, C. J. Oh, P. Su, et al.

L. R. Graves, H. Choi, W. Zhao, C. J. Oh, P. Su, T. Su, D. W. Kim, "Model-free optical surface reconstruction from deflectometry data," Proc. SPIE 10742, Optical Manufacturing and Testing XII, 107420Y (14 September 2018); doi: 10.1117/12.2320745

Event: SPIE Optical Engineering + Applications, 2018, San Diego, California, United States

# Model-free optical surface reconstruction from deflectometry data

L. R. Graves[a], H. Choi[a], W. Zhao[b], C. J. Oh[a], P. Su[c], T. Su[d], D. W. Kim[a,e*]

[a]College of Optical Sciences, Univ. of Arizona, 1630 E. University Blvd., Tucson, AZ USA 85721
[b]The Institute of Optics and Electronics, Chinese Academy of Sciences, Chengdu 610209, China
[c]ASML Corporation, 77 Danbury Road, Wilton, TC 06897 USA
[d]KLA-Tencor Corporation, 3 Technology Dr., Miltipas, CA 95035, USA
[e]Steward Observatory, University of Arizona, 933 N. Cherry Ave., Tucson, AZ 85719, USA

## ABSTRACT

Deflectometry is a metrology method able to measure large surface slope ranges that can achieve surface reconstruction accuracy similar to interferometry, making it ideal for freeform metrology. While it is a non-null method, deflectometry previously required a precise model of the unit under test to accurately reconstruct the surface. However, there are times when no such model exists, such as during the grinding phase of an optic. We developed a model-free iterative data processing technique which provides improved deflectometry surface reconstruction of optics when the correct surface model is unknown. The new method iteratively reconstructs the optical surface, leading to a reduction in error in the final reconstructed surface. Software simulations measuring the theoretical performance limitations of the model-free processing technique as well as a real-world test characterizing actual performance were performed. The method was implemented in a deflectometry system and a highly freeform surface was measured and reconstructed using both the iterative technique and a traditional non-iterative technique. The results were compared to a commercial interferometric measurement of the optic. The reconstructed surface departure from interferometric results was reduced from 44.39 µm RMS with traditional non-iterative deflectometry down to 5.20 µm RMS with the model-free technique reported.

**Keywords:** Deflectometry, model-free, metrology, freeform

## INTRODUCTION

As the use of freeform optics in optical systems increases, there is a growing demand for accurate and dynamic metrology systems. Two popular optical tests methods that are used for freeform metrology are deflectometry and interferometry [1, 2]. Interferometry requires a null configuration for accurate results. This poses a challenge for freeform optics, as the null optics will typically have to be custom computer generated holograms (CGHs) [3]. While CGHs are extremely useful, they are expensive and only work for one null configuration. Deflectometry, a non-null test method, has been used to provide accurate metrology of standard to freeform optics [4–6]. A deflectometry test relies on having a source at a defined position. The ray emitted from the source is deflected by the unit under test (UUT) and is recorded by a detector. This allows for surface slope calculations of the UUT, and the process can be thought of as a reverse Hartmann test. By recording the ray start and end location, the slope on the UUT which deflected the ray is calculated. This slope calculation is typically done in a ray trace program, and the slope calculation relies on having an accurate estimation of where the ray was deflected by the UUT [5-6]. To minimize the error in the slope calculation an accurate model of the UUT is required for the ray trace process. However, it is not always possible to have an accurate surface model of the UUT; an example of this is during the grinding phase of an optic where the root mean square (RMS) surface shape error from an ideal surface can change by millimeters between runs. In lacking an accurate surface model of the UUT, significant error in the final reconstruction model can develop, particularly in the low to mid surface shapes [5]. There are limited methods for reconstructing deflectometry data when an accurate surface model is unknown, and all require significant user input. A standard approach when no accurate model exists is to simply model the UUT as a flat, recognizing that the final reconstruction map's low-mid order shape values have high uncertainty. More advanced approaches such as an iterative system parameter optimization process [7] and a rapid reconstruction method using a non-zonal parameter dependent integration to improve the initial UUT model followed by a successive over relaxation zonal integration [8, 9] can lead to improved reconstruction accuracy.

*letter2dwk@hotmail.com

Optical Manufacturing and Testing XII, edited by Ray Williamson, Dae Wook Kim,
Rolf Rascher, Proc. of SPIE Vol. 10742, 107420Y · © 2018 SPIE
CCC code: 0277-786X/18/$18 · doi: 10.1117/12.2320745

One primary limitation of these methods however is the demand for involved used input. We developed a model free iterative deflectometry (MID) reconstruction approach which avoids the need for any user input model [10]. The MID process begins always with a flat as the starting shape assumption and reconstructs the surface, which then serves as the surface model for the next iteration. This process is repeated until a final reconstructed surface is converged upon. By utilizing a continuously updating surface model, the MID method achieves improved accuracy in the low to mid spatial frequencies in the reconstruction map without any user input beyond the raw deflecomtetry data. In this paper we present a test of a freeform optic and the reconstruction results using the MID technique, which is described in detail in our previous publication [10]. A simulation is also presented which explores the influence the geometric position uncertainty in the system has on the final reconstruction map.

## METHODOLOGIES

The raw input data for the MID approach does not differ significantly from traditional deflectometry processing methods. The Cartesian coordinates in object space (UUT) of the source and the camera, which are defined as matrices S and C respectively, must be known to high accuracy and must be input to the software. For the UUT itself, the MID approach always starts by defining the model as a flat, referred to as matrix $U^0$. The UUT clear aperture diameter must be input and, to bound piston of the model, one point on the UUT, $u^k(x,y,z)$, must be measured to determine its Cartesian coordinate in object space as well as what pixel on the camera is measuring it. The final input for the MID approach are the ray pointing vectors of the camera detector pixels, defined as vector R. Using these inputs, the MID process runs for a total of t = 0:N iterations and results in a final reconstruction surface $U^N$. The overall process is shown in figure 1.

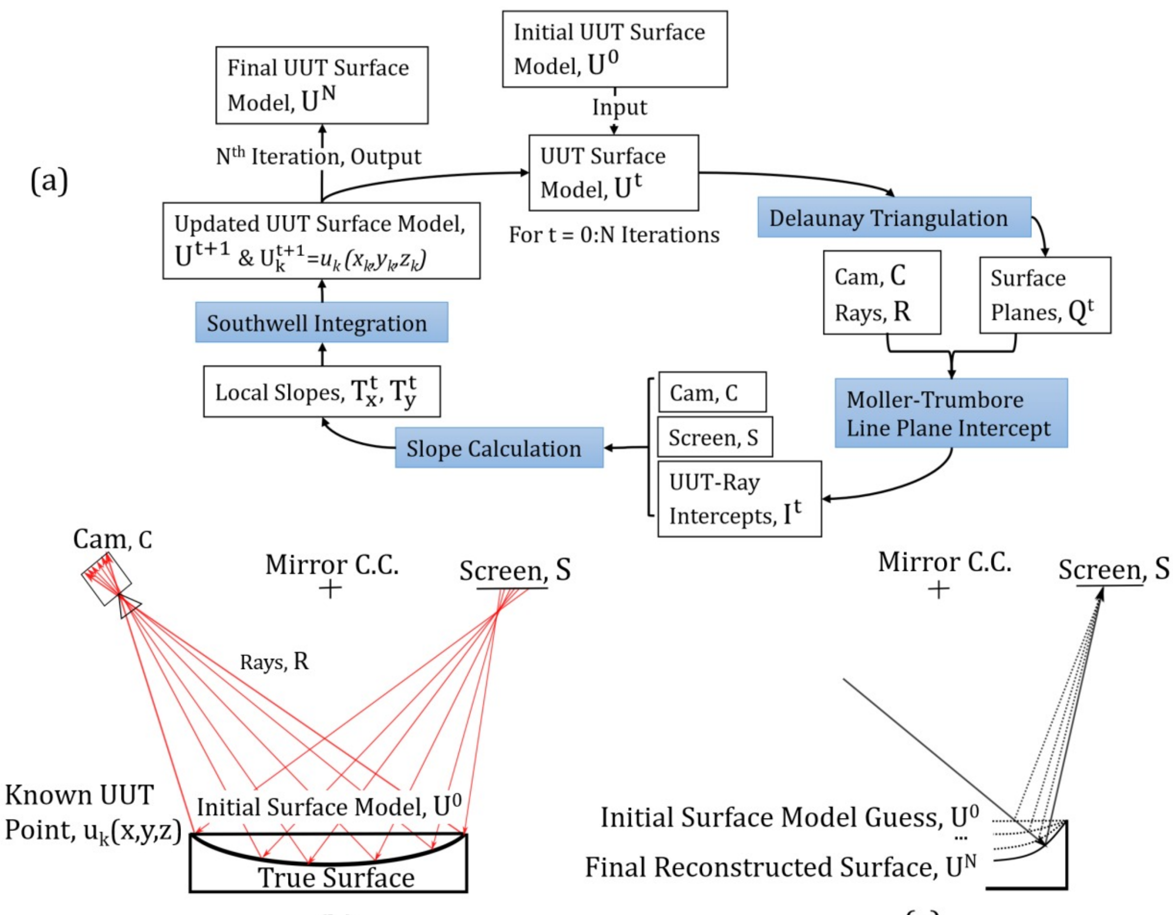


Figure 1. Using the initial flat surface model, $U^0$, the MID process iterates N times and generates the final surface reconstruction map $U^N$ (a). With a traditional non-iterative approach when the UUT model is incorrect the ray intercepts are calculated at the plane of $U^0$ (b). Using the MID method, the true surface can be converged upon (c) [10].

During the MID process the UUT model is first segmented into surface planes, defined as matrix $Q^t$ , using a Delaunay triangulation [11]. Rays are then traced from the detector and the intercept locations, defined as matrix $I^t$, calculated using a Möller–Trumbore algorithm [12]. The combined Delaunay/ Möller–Trumbore (DMT) process allows for highly accurate slope calculations at every iteration. The Delaunay process takes the discrete surface points, which are defined by mapping the camera pixels to the UUT surface model and segments them into unique planes that are well-shaped triangles and satisfy a nearest-neighbor relationship. Coupled with the Möller–Trumbore algorithm, which performs a highly efficient rapid ray-plane intercept calculation, the exact ray intercept coordinate in the surface planes is determined in 3D space. The combined DMT process linearly increases in total processing time while an improvement in accuracy exponentially decays with respect to the number of camera pixels used. The process is demonstrated in figure 2 [10].

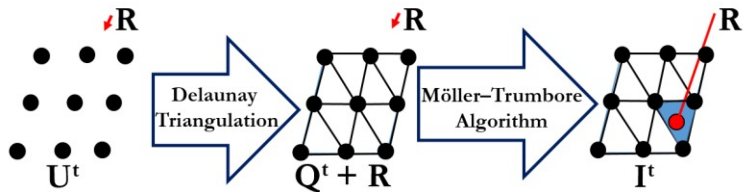


Figure 2. Surface points $U^t$ are segmented into triangular planes, $Q^t$, using a Delaunay algorithm. The ray intercepts, $I^t$, are then calculated using a Möller–Trumbore algorithm.

The local slopes at the UUT model surface in the x and y directions, defined as matrices $T_x^t$ and $T_y^t$ respectively, are calculated using the ray start and end locations, C and S, and the intercept coordinates. The local slopes are then integrated using a standard Southwell integration [13] to reconstruct the surface model. The process is iterated, with a new reconstructed model $U^t$, being output at each iteration for a total of N iterations, at which point the final reconstructed model is output, referred to as model $U^N$.

In a previous paper, the performance of the MID approach was compared to a traditional non-iterative reconstruction method for deflectometry data [10]. The optic tested was a bare glass surface with freeform departure in all directions and had a radius of curvature (RoC) of 200 mm and a clear aperture diameter of 100 mm. The surface was generated using a magnetorheological finishing (MRF) method which imparted a spiral pattern unto the surface. As a reference comparison the UUT was measured using a commercial interferometer, a Zygo Verifire™ MST. A Zygo F/1.75 sphere was used as the reference optic for the interferometer. The interferometer cannot accurately measure piston, tip, tilt, and power, and thus these terms were dismissed in all measurements, both interferometric and from the deflectometry test. Due to the steep freeform departure and the lack of a custom CGH for the test there was high fringe density even at best null configuration which resulted in partial surface reconstruction error and missing data in the final surface. Figure 3 shows the best null configuration obtained in the interferometric test and highlights the complex fringe pattern and the challenges associated with measuring the optic [10].

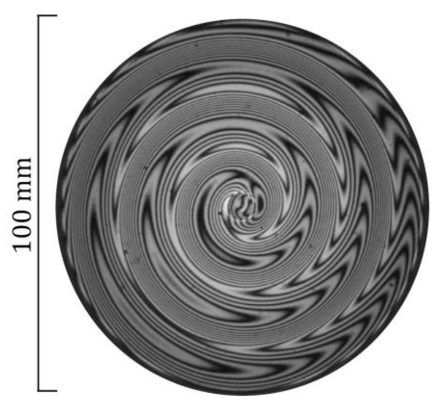


Figure 3. The UUT had a spiral pattern imparted on the surface which made obtaining an interferometric null impossible across the entire surface. High fringe density resulted in low modulation which made some areas on the map unmeasurable.

To obtain a deflecomtetry measurement of the UUT a SCOTS type system was utilized. The system consisted of an LCD monitor which acted as the phase shifting source and an off the shelf camera. The UUT was mounted onto a rotation stage below the screen and camera, which were located near the center of curvature of the UUT. All components were securely mounted on a breadboard which allowed for their positions to be maintained throughout testing. To measure the position of all components a coordinate measuring machine (CMM) was used with a touch tip probe, which provided position accuracy to ±10 µm. The body edges of the camera were measured, and the detector plane was located relative to the camera body using technical drawings. For the screen, the monitor edges were measured, and a plane was fit which defined the source. Finally, the center of rotation on the surface of the UUT was measured, which served as the known coordinate, $u_k$ $(x_k,y_k,z_k)$ and as the global zero coordinate in x, y, and z. This was related to the camera pixel measuring the known coordinate, pixel p(x,y,z). The full system parameters are listed below in table 1.

Table 1. Deflectometry Test System parameters

| Camera Parameters | |
|---|---|
| Manufacturer | Point Grey |
| Model | FL3-U3-32S2M-CS |
| Resolution | 2080x1552 |
| Chroma | Mono |
| Pixel Pitch | 2.5 µm |
| **Source Parameters** | |
| Manufacturer | Mimo Monitors |
| Model | Mimo UM-760F |
| Resolution | 1024x600 |
| Pixel Pitch | 150 µm |
| **Mirror Parameters** | |
| Manufacturer | Optimax Systems, Inc |
| Method | MRF |
| Surface | Bare Glass |
| Diameter of Optic | 100 mm |
| Radius of Curvature | 200 mm |

For system calibration and to determine the pointing vectors of the camera pixels the ray intercept locations of the camera pixels were measured at two locations. The camera was positioned at location c(x,y,z) and fixed in place. A screen was then placed facing the camera at location $l_1(x,y,z)$. The screen pixels were then activated to determine which screen pixels were being measured by each camera pixel. The screen was then shifted axially along the camera pointing direction to a second location, $l_2(x,y,z)$, and the process was repeated. By measuring the screen intercept coordinates of the camera pixels at two locations the pointing vectors for every camera pixel were recorded. All positions, c(x,y,z), $l_1(x,y,z)$, and $l_2(x,y,z)$, were measured using a CMM which was accurate to ± 10 µm. The test setup of the ray pointing vector calibration process is shown below in figure 4 [10].

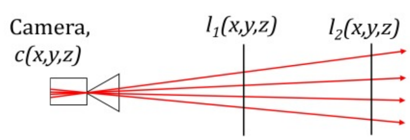


Figure 4. The ray path of all camera pixels was determined by measuring the ray intercept at two locations, $l_1$ and $l_2$.

To obtain the raw deflectometry data the screen displayed a total of eight fringes, four in the x and four in the y directions, while the camera measured the reflected signal from the UUT. To reduce systematic error, the UUT was clocked 36 times, with a 10° clocking each time for a full rotation and was measured at each position. This allowed for a rotation calibration to be performed [14]. After the raw data was obtained the surface was reconstructed in three ways. First, the MID method was performed, using a total of six iterations to reconstruct the surface. Second, a traditional non-iterative reconstruction method was performed using the same raw data, in which (1) a flat surface was assumed as the UUT model and (2) a 200 mm RoC base sphere model was assumed. For all the methods the phase maps were unwrapped using a four-bucket unwrapping algorithm to determine the screen coordinates, which were used for the local slope calculations. The local slopes were integrated using a Southwell integration to obtain a reconstructed surface. The clocked measurements were reconstructed and averaged to create systematic error maps which were removed from the reconstructed surfaces to generate the final reconstruction maps for the MID method and the two traditional techniques, referred to as $MID_6$, $MB_{flat}$, and $MB_{sphere}$ respectively. These maps were analyzed, and low order standard Zernike terms were fit to the data to compare to the interferometric map, referred to as INT. The missing data regions in the INT map were not considered in the comparison to avoid extrapolation.

To complement the results of the paper a simulation of the test setup was performed, in which the system was modeled as measured and the screen and camera positions were modeled with ±10 µm uncertainty as well as a tip/tilt/rotation uncertainty of 1 mrad. The simulation was created to model the expected error effects in the final reconstruction surface due to the geometric uncertainty of the real test setup. Using the test setup uncertainty values described, the measurement was simulated, and the surface was reconstructed using the MID method for six iterations. The error between the reconstructed surface map and the ideal surface was calculated and low order standard Zernike terms Z5:Z11 were fit to the error maps. This allowed for an estimation of the amount of error that could reasonably be expected in the final reconstruction results for the real test based on the position uncertainties that existed in the test measurement.

## RESULTS

The simulation was constructed in Matlab in which an ideal sphere modeled on the previously measured optic served as the UUT, with a radius of curvature of 200 mm and a diameter of 100 mm. The position of the screen and camera were modeled on the measured position of the test performed in the previous paper. Using the previously measured ray pointing vectors, a ray trace was performed which traced the rays from the camera pupil to the modeled UUT, and finally to the screen plane. Using this data, which represented the modeled raw output data we expect from a deflectometry test, the surface was reconstructed using the MID method. For no input error the MID method converged to a perfect reconstruction (limited by machine precision). The camera position was then modeled with a 10 µm error in the x, y, and z positions, as well as a tip, tilt, and rotation error of 1 mrad. Similarly, the screen was modeled with a 10 µm error in the x, y, and z positions and a tip, tilt, and rotation error of 1 mrad. These values represented the uncertainty in the position knowledge of the components in the previous paper [10]. The surface was then reconstructed using the MID approach and the difference in the reconstructed surface with geometric error induced versus the perfect reconstruction surface was determined. Standard Zernike terms 5:11 were fit to the difference map and a root-sum-square (RSS) was calculated for the error from the various configurations to determine the total error attributable to the geometric uncertainty. The results of the surface error in the reconstruction of the simulations are shown below in table 2 and table 3.

Table 2. Screen Uncertainty Simulation Reconstruction Error

| Zernike Terms | 10 µm X Pos. Error (µm) | 10 µm Y Pos. Error (µm) | 10 µm Z Pos. Error (µm) | 1 mrad Tip Error (µm) | 1 mrad Tilt Error (µm) | 1 mrad Rotation Error (µm) | RSS Value (µm) |
|---|---|---|---|---|---|---|---|
| Z5 | 0.003 | -1.497 | -0.042 | 0.031 | -0.002 | -0.001 | **1.50** |
| Z6 | 1.471 | 0.002 | 0.203 | 0.001 | 0.034 | 0.002 | **1.49** |
| Z7 | 0.005 | 0.603 | 0.010 | 0.003 | 0.001 | 0.001 | **0.60** |
| Z8 | 0.576 | 0.007 | 0.038 | 0.002 | 0.002 | 0.001 | **0.58** |
| Z9 | 0.028 | 0.161 | 0.031 | 0.078 | -0.015 | -0.002 | **0.18** |
| Z10 | -0.580 | 0.161 | -0.102 | 0.018 | 0.078 | 0.002 | **0.62** |
| Z11 | 0.207 | 0.171 | 0.152 | 0.170 | 0.170 | 0.170 | **0.38** |

Table 3. Camera Uncertainty Simulation Reconstruction Error

| Zernike Terms | 10 µm X Pos. Error (µm) | 10 µm Y Pos. Error (µm) | 10 µm Z Pos. Error (µm) | 1 mrad Tip Error (µm) | 1 mrad Tilt Error (µm) | 1 mrad Rotation Error (µm) | RSS Value (µm) |
|---|---|---|---|---|---|---|---|
| Z5 | -0.006 | 4.119 | -0.120 | -0.001 | -0.001 | -0.001 | **4.12** |
| Z6 | -4.093 | 0.000 | 0.600 | 0.000 | 0.000 | 0.000 | **4.14** |
| Z7 | -0.008 | -1.311 | 0.055 | 0.001 | 0.001 | 0.001 | **1.31** |
| Z8 | -1.253 | -0.008 | 0.261 | 0.001 | 0.001 | 0.001 | **1.28** |
| Z9 | -0.203 | -1.033 | 0.051 | 0.000 | 0.000 | 0.000 | **1.05** |
| Z10 | 1.787 | -0.313 | -0.177 | 0.004 | 0.004 | 0.004 | **1.82** |
| Z11 | 0.092 | 0.165 | -0.479 | 0.170 | 0.170 | 0.170 | **0.56** |

The raw data from the deflectometry measurement of the UUT was reconstructed using the three methods, MID and the traditional non-iterative technique. The reconstructed surface maps were compared to the interferometric map and the difference between the surfaces was determined. The difference between the reconstruction maps had low order standard Zernike terms up to Z11 fit to the data. The first four Zernike terms, piston, tip, tilt, and power were not considered in the fit. The results are shown below in table 4.

Table 4. Low Order RMS Normalized Zernike Term Difference between Reconstructed and Interferometric Surface Maps

| Zernike Term | $MID_6$ (µm) | $MB_{flat}$ (µm) | $MB_{sphere}$ (µm) |
|---|---|---|---|
| Z5, Oblique Astigmatism | 0.76 | 1.90 | 0.42 |
| Z6, Vertical Astigmatism | -5.12 | -44.28 | -15.80 |
| Z7, Vertical Coma | -0.36 | -1.98 | -0.40 |
| Z8, Horizontal Coma | -0.10 | 0.55 | 0.11 |
| Z9, Vertical Trefoil | 0.32 | 1.01 | 0.25 |
| Z10, Oblique Trefoil | -0.05 | 0.29 | 0.06 |
| Z11, Spherical | 0.04 | 0.63 | 0.17 |
| Z5:Z11 Total RMS Diff | 5.20 | 44.39 | 15.80 |

For low order terms Z5-Z11, the total Zernike term root-mean-square (RMS) departure from the INT map for the $MID_6$, $MB_{flat}$, and $MB_{sphere}$ surfaces were 5.20 µm, 44.39 µm, and 15.80 µm, respectively. Based on the low order departure from INT, the MID method provides close to an order of magnitude improvement in reconstruction accuracy when compared to a traditional non-iterative approach with a flat as the model. When observing the reconstruction maps the astigmatism and coma mismatch between INT and the other reconstruction methods is apparent. The reconstruction maps with increasing Zernike terms removed are shown below in figure 5.

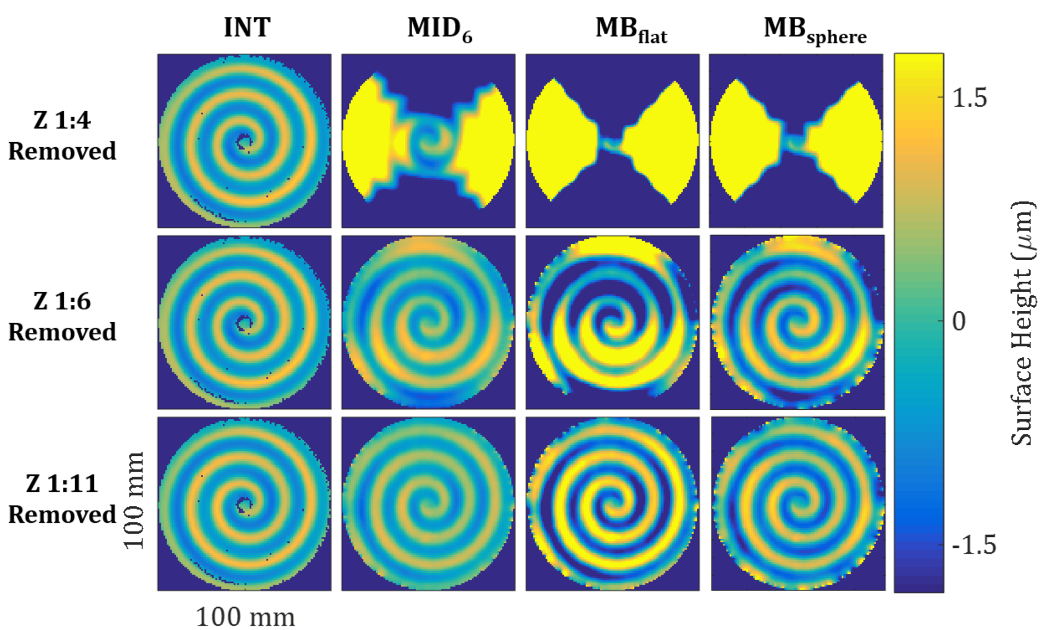


Figure 5. The interferometric surface map of the UUT (1st column), MID technique with 6 iterations (2nd column), and non-iterative traditional reconstruction with a flat UUT model (3rd column) and a 200 mm RoC base sphere model (4th column) method had Zernike terms 1-4 (top row), 1-6 (middle row), and 1-11(bottom row) removed to compare error contribution from low spatial frequency. Please note missing data regions in the interferometric surface map resulted from high fringe density in the measurement due to not having a custom CGH [10].

## DISCUSSION

The MID approach produced a reconstruction map which more closely matched the interferometric measurement as compared to a traditional non-iterative reconstruction approach when no accurate model of the UUT exists. The improvement is particularly apparent at low order surface shapes, such as astigmatism and coma, where deflectometry traditionally suffers in reconstruction accuracy. However, there are still residual low order spatial features present in both MID and traditional non-iterative reconstruction approaches which were not present in the interferometric map. This is partly explained by the geometric uncertainties present in the deflectometry measurement. Any geometric error leads to significant reconstruction error in the final map. Most of the astigmatism and coma present in the final map from the MID method was predicted from the simulation of the test setup. This residual error can be reduced by using more advanced calibration methods to reduce geometric uncertainty.

Overall, the MID method was able to significantly reduce the low order terms as compared to the non-iterative approach, as well as demonstrating a capability to measure the large dynamic range of the UUT. This is particularly clear when considering the interferometric map of the UUT, which without a custom CGH struggled to achieve an ideal null, and thus resulted in missing data in the final map due to high fringe density.

## CONCLUSION

The MID approach utilizes an iterative reconstruction method which leverages a Delaunay/ Möller–Trumbore algorithm to achieve improved reconstruction accuracy of raw deflectometry data. The approach can readily be applied to a deflectometry data processing package and can also be used on previously measured data. When testing a freeform bare glass UUT the MID method resulted in a final reconstructed surface map which more closely matched an interferometric measurement of the surface as compared to a traditional non-iterative deflectometry reconstruction approach of the same raw data. The improvement in accuracy is particularly apparent at low order spatial features, where traditional non-iterative deflectometry approaches struggled when no accurate UUT model was known. The residual errors in the final reconstruction approach were predicted by a simulation of the test which accounted for the geometric uncertainty of the positions of the hardware components. Thus, by improving calibration and hardware methods a further improvement in accuracy can be expected.

## ACKNOWLEDGEMENT

This research was made possible in part by the II-VI Foundation Block-Gift Program, the Technology Research Initiative Fund Optics/Imaging Program, the Post-processing of Freeform Optics project supported by the Korea Basic Science Institute, the Friends of Tucson Optics (FoTO) Endowed Scholarships in Optical Sciences, and we thank Optimax Systems for providing the freeform UUT.

## REFERENCES

[1] Martin, B., Burge, J., Miller, S., Warner, S., and Zhao, C., "Fabrication and Testing of 8.4 m Off-Axis Segments for the Giant Magellan Telescope" Frontiers in Optics 2008/Laser Science XXIV/Plasmonics and Metamaterials/Optical Fabrication and Testing, OSA Technical Digest (CD) (2008).

[2] Oh, C.J., Lowman, A., Smith, G., Su, P., Huang, R., Su, T., Kim, D.W., Zhao, W., Zhou. P., and Burge, J., "Fabrication and testing of 4.2m off-axis aspheric primary mirror of Daniel K. Inouye Solar Telescope," Proc. SPIE 9912 (2016).

[3] Dubin, M.B., Su, P., and Burge, J., "Fizeau interferometer with spherical reference and CGH correction for measuring large convex aspheres," Proc. SPIE 7426 (2009).

[4] Kim, D.W., Oh, C.J., Lowman, A., Smith, G., Aftab, M., and Burge, J., "Manufacturing of super-polished large aspheric/freeform optics," Proc. SPIE 9912 (2016).

[5] Huang, R., "High Precision Optical Surface Metrology using Deflectometry," Academic, (2015).

[6] Kim, D.W., Aftab, M., Choi, H.C., Graves, L., and Trumper, I., "Optical Metrology Systems Spanning the Full Spatial Frequency Spectrum," presented at the Frontiers in Optics, p. FW5G.4. (2016).

[7] Olesch, E., Faber, C., and Häusler, G., "Deflectometric Self-calibration for arbitrary specular surfaces" in DGaO Proc. 112 Academic (2011).

[8] Zhou, T., Chen, K., Wei, H., and Li, Y., "Improved method for rapid shape recovery of large specular surfaces based on phase measuring deflectometry," Appl. Opt. 55, 2760-2770 (2016).
[9] Zhang, H., Han, S., Liu, S., Li, S., Ji, L., and Zhang, X., "3D shape reconstruction of large specular surface," Appl. Opt. 51, 7616-7625 (2012).
[10] Graves, L.R., Choi, H., Zhao, W., Oh, C.J., Su, P., Kim, D.W., “Model-free deflectometry for freeform optics measurement using an iterative reconstruction technique,” Opt. Letters 43, (2018).
[11] Cheng, S., Dey, T., and Shewchuk, J., [Delaunay Mesh Generation], CRC Press, (2013).
[12] Möller, T., and Trumbore, B., “Fast, Minimum Storage Ray-Triangle Intersection,” J. of Graph. Tools, V 2, 21–28, (1997).
[13] Southwell, W.H., "Wave-front estimation from wave-front slope measurements," J. Opt. Soc. Am., JOSA 70, 998–1006 (1980).
[14] Evans, C., Hocken, R., and Estler, W., “Self-Calibration: Reversal, Redundancy, Error Separation, and ‘Absolute Testing’,” CIRP Annals V 45, Issue 2, 617-634, (1996).